

S. RANGREJ^{1*}, S. PANDYA¹, J. MENGHANI¹

INVESTIGATION ON THE MICROSTRUCTURE, MICROHARDNESS AND TENSILE STRENGTH OF STIR-CASTED A713-TiB₂ COMPOSITES

A parametric experimental investigation has been conducted to investigate effects of stir casting process parameters on recently developed A713-TiB₂ composites. The manufacturing process involved varying the stirring time (5, 10, and 15 minutes) and speed of stirring (500, 600 & 700 rpm). The microstructure and mechanical properties of the manufactured composites were evaluated by analyzing the effects of the varying stirring speeds and times. The analysis techniques used include optical microscopy (OM), scanning electron microscopy (SEM), micro-hardness and tensile testing. Grain size analysis of the as-cast MMCs revealed that coarser grain structure was observed at lower stirring time and lower speed. Finer grain structure was achieved by increasing stirring time and speed. Microhardness and tensile strength was observed to be affected by both stirring speed and stirring time, as demonstrated by the test results. The uniform dispersion was attained when stirring was done at 600 rpm for 10 minutes. Further increase in stirring speed and stirring time leads to the reduction in microhardness and tensile strength. In the present study, the relationship between the microstructure and mechanical properties of the A713-TiB₂ composite and the processing parameters such as stirring speed and stirring time have been investigated.

Keywords: A713-TiB₂ composites; Microstructure; Microhardness; Stir casting

1. Introduction

Aluminum matrix composites (AMCs) – aluminum alloys reinforced with a variety of particulates – have been the focus of extensive research over the past two decades due to their exceptional characteristics [1]. In many contexts, conventional monolithic aluminium alloys are unable to satisfy the ever-increasing demand for products with high levels of performance. AMCs could replace aluminium alloys because they are stiffer, more resistant to wear, stronger, and have a low coefficient of thermal expansion [2]. As a whole, the use of AMCs is on the rise in several sectors, including the aviation, automotive, marine, and nuclear industries [3,4]. In AMCs, aluminium alloys reinforced with different reinforcement particles have been developed by various manufacturing routes. These particles include fly ash [5], TiB₂ [6], SiC [7], Al₂O₃ [8], AlN [9], B₄C [10], SiO₂ [11], Si₃N₄ [12], TiC [13], and ZrB₂ [14]. Among them, TiB₂ particles have widespread popularity owing to its excellent stiffness [15], hardness [16], and wear resistance properties [17]. In addition to that TiB₂ is thermodynamically stable in aluminum and does not react with aluminum matrix, and also facilitates the refining of grains by acting as a nucleating agent [18].

The synthesis of AMC materials can be accomplished through a variety of methods, including liquid metal infiltration, squeeze casting [19], mixing techniques like compocasting and stir casting [20], powder metallurgy [21], and spray co-deposition [22]. Among all commercially-used fabrication methods, stir casting offers the greatest cost savings for synthesizing AMCs because of its simplicity, adaptability to conventional shape casting foundry processes, and suitability for high-volume production. Furthermore, the AMC billets made in this way are amenable to further shaping by extrusion, rolling, etc. [23]. Various challenges with the stir casting method include micro-porosity, uneven distribution of particles, chemical reactions at the interface, and the disintegration of particular ceramic particles [24]. Therefore, it is crucial to select the best combination of process parameters in order to attain good combination of properties of AMCs. Even though there is a large number of research publication available on AMC production, very few studies have been examined the effects of varying process parameters [25-34].

Arunachalam et al. [25] found that increasing stirring speed improves particle distribution homogeneity in Al-Si7Mg/Alumina AMCs. As reported by Prabu et al. [26], there is observed poor particle dispersion and clustering in A384/SiC AMCs

¹ DEPARTMENT OF MECHANICAL ENGINEERING, SVNIT, SURAT, GUJARAT-395007, INDIA

* Corresponding author: shyamrang24@gmail.com



when the stirring speed was reduced along with the stirring time. Hasim et al. [27] found that wettability between A359 matrix and SiC particles improved with increasing the stirring speed. Sasaki et al. [28] examined a graphical model of glycerin, which exhibits certain characteristics with AZ91D magnesium alloy, and concluded that the gas entrapment is influenced by the blade's distance from the liquid's surface, rotating speed of the stirrer blade, and the duration for which the blade is stirred. Krishnan et al. [29] observed that it was difficult to achieve a uniform dispersion of the reinforcing particles into the matrix. It was concluded that the uniform dispersion of reinforcement into the matrix can be achieved through the careful selection of the blade parameters. Sozhamannan et al. [30] examined the microstructure, physical properties and mechanical properties of fabricated AMC to determine the effect of process parameters. It was observed that particle dispersion and viscosity of molten aluminium affected by holding time. The hardness of fabricated composites varied linearly with processing temperature. Using a SiC reinforced aluminium matrix composite, Zhang et al. [31] investigated effects of the stirring time, stirring speed and processing temperature on microstructural characterization and particle dispersion. Li-na et al. [32] fabricated hybrid aluminium composites reinforced with SiC_p and ABO_w particles and reported that microstructure and mechanical properties AMCs were found to be more uniform at higher stirring time and lower stirring temperature. The porosity content of A356/Al₂O₃ AMCs was found to increase with stirring time, as reported by Akbari et al. [33]. According to Khosravi et al. [34], the porosity content of A356/ SiC AMCs rises in conjunction with the stirring speed and casting temperature.

Al-Zn (A713) Cast alloy is low weight alloy used for a wide range of applications in the automotive and aerospace industries. A713 alloy castings have higher strength. It also exhibits excellent tribological and damping properties. However, there are limited number of publications about structure and properties of A713 matrix based composites [6]. The primary objective of this study was to analyse the relationship between stirring speed and time in facilitating the uniform distribution of TiB₂ reinforcement throughout the A713 alloy matrix. In the open literature, the influence of time duration during stirring and speed of stirring for this kind of composite system has not been explored. Therefore, the purpose of this study is to examine the effect of stirring speed and stirring duration on the microstructure, microhardness, and tensile strength of TiB₂ reinforced A713 composites.

2. Methods and Materials

In this research, the cast alloy of Al-Zn (A713 alloy) is utilised as matrix material because of its superior castability and automotive applications. The chemical composition of matrix A713 alloy is listed in TABLE 1. Stir casting process was used in the preparation of the composites. The stir casting setup

is shown in the Fig. 1. A713 matrix alloy first heated above its liquidus temperature in a stir casting furnace. The molten metal is stirred between speeds of 500-700 rpm with an impeller made of stainless steel. The plan of experiments of the study is shown in TABLE 2. The blades of the impeller were built with a view to generate a vortex in order to accomplish the mixing of the particles. The stirrer blade were coated with graphite to decrease chances of dissolution of blades in the molten metal. The matrix alloy was melted, and then the stirrer was lowered into the molten metal to disperse reinforcement particles. The speed of the stirrer was kept in the range of 500-700 rpm. In this investigation, Particles of TiB₂ with a size range of 10-20 microns were employed. The determined amount (2 wt.%) of TiB₂ was heated in muffle furnace at 550°C for 1 hour. After that heated particles are being added into molten matrix at a consistent rate. The stirring time was recorded up to three levels 5, 10, and 15 minutes after the addition of TiB₂. The high carbon steel die is used for the casting, which had been preheated to around 300°C. After the proper dispersion, molten metal is poured into the hot die using a bottom pouring attachment. Fig. 2 shows the stir-cast castings of (A713-2%TiB₂) MMCs.

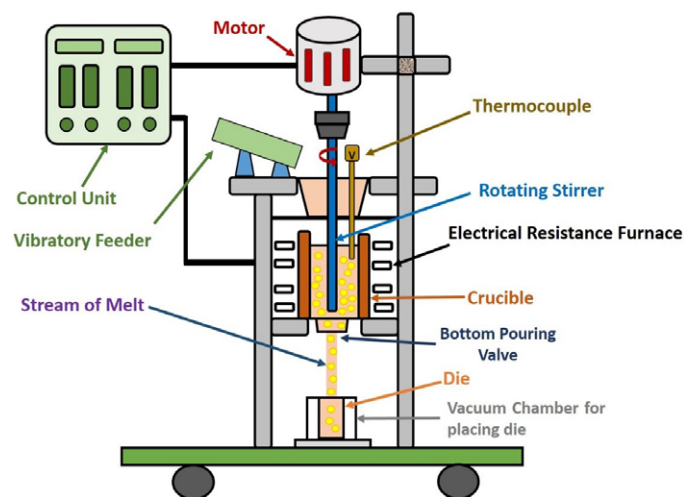


Fig. 1. Stir casting setup



Fig. 2. Fabricated A713-2% TiB₂ MMCs

TABLE 1
Composition of aluminium (A713) alloy (wt.%)

Zn	7.76
Mn	0.401
Cu	0.495
Si	0.438
Fe	0.685
Mg	0.499
Al	Balance

TABLE 2
Plan of experiments

Sr. No.	Sample ID	Stirring speed (rpm)	Stirring time (minutes)
1	500-5	500	5
2	500-10	500	10
3	500-15	500	15
4	600-5	600	5
5	600-10	600	10
6	600-15	600	15
7	700-5	700	5
8	700-10	700	10
9	700-15	700	15

3. Results and discussions

3.1. Microstructural characterization

The homogeneous dispersion of reinforcement particles into matrix material is necessary to enhance the mechanical properties of stir-cast composites. To achieve particle uniformity in the matrix, it is required to investigate and optimised the stir casting process parameters. Therefore, it is required to evaluate the effect of speed of stirring and stirring time on microstructure of composites to investigate dispersion of reinforced particles in MMCs.

Grain size analysis was carried out using the BIOVIS Material plus software in accordance with ASTM E112. It is seen from the grain size analysis that coarser grains with an average grain size of 29.2 microns are observed in optical micrograph (Fig. 3) of A713 matrix alloy. This is due to dominant homogeneous nucleation and higher degree of supercooling. Super cooled liquid metal during solidification results into formation of platelets until effect of supercooling is set off. Thus, platelets are formed

within solidified metal. Formation of platelets further promotes coarse grain structure. Optical micrographs (Fig. 3) show that the needle type of platelets causes the development of shrinkage depressions because the liquid metal can't flow into the gaps between the branching platelets due to the larger main dendrite arm length. Liquid metal flow is blocked between two nearby primary platelet arms due to narrow gap. This leads to formation of micro-shrinkage cavities when the entrapped liquid within the gap between two platelet arms solidifies due to lack of supply of liquid metal to compensate solidification shrinkage [35].

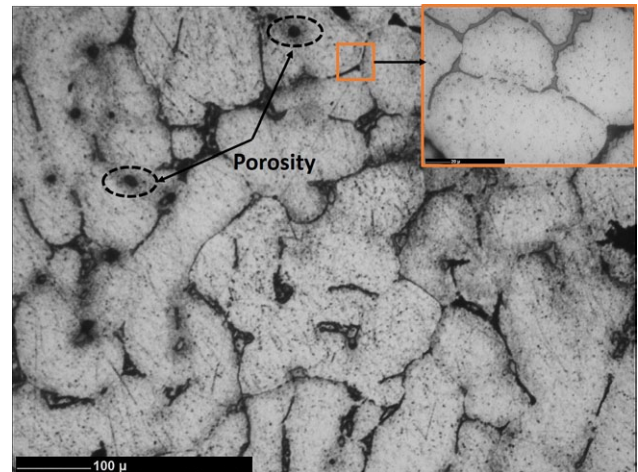


Fig. 3. Microstructure of as cast A713 matrix-alloy

The optical micrographs of (A713+2% TiB₂) MMCs fabricated at different levels of stirring speeds and different levels of stirring time are shown in Figs. 4-6. It is seen that the incorporation of TiB₂ particles into A713 alloy has resulted in the transformation of the coarse grains of matrix material into finer and better equiaxed grains. This is due to addition of TiB₂ particles. Addition of TiB₂ particles promotes heterogeneous nucleation (Fig. 4-6). Due to heterogeneous nucleation grain size in solidified metal decreases. The extent of formation of platelets also decreases restricting formation of coarser grains which may be attributed to presence of TiB₂ particles. Fig. 4-6 shows addition of TiB₂ reinforcements and subsequent formation of porosity and inferior dendrites. The inadequate formation of Zn phase may be the cause of the inferior dendrites [36]. Rajan et al. [37] have also found similar results.

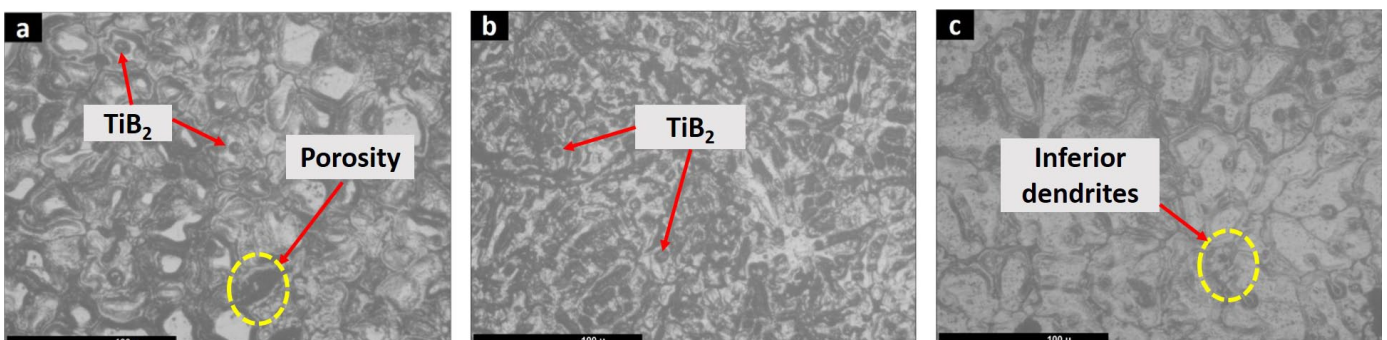


Fig. 4. Influence of stirring time on microstructure of (A713+2% TiB₂) composite cast at stirring speed of 500 rpm: (a) 5 min (b) 10 min (c) 15 min

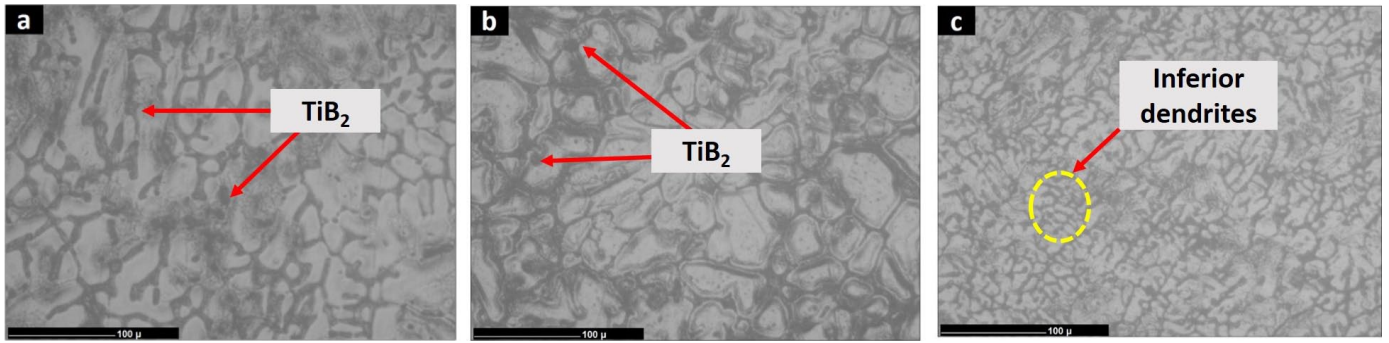


Fig. 5. Influence of stirring time on microstructure of (A713+2% TiB₂) composite cast at stirring speed of 600 rpm: (a) 5 min (b) 10 min (c) 15 min

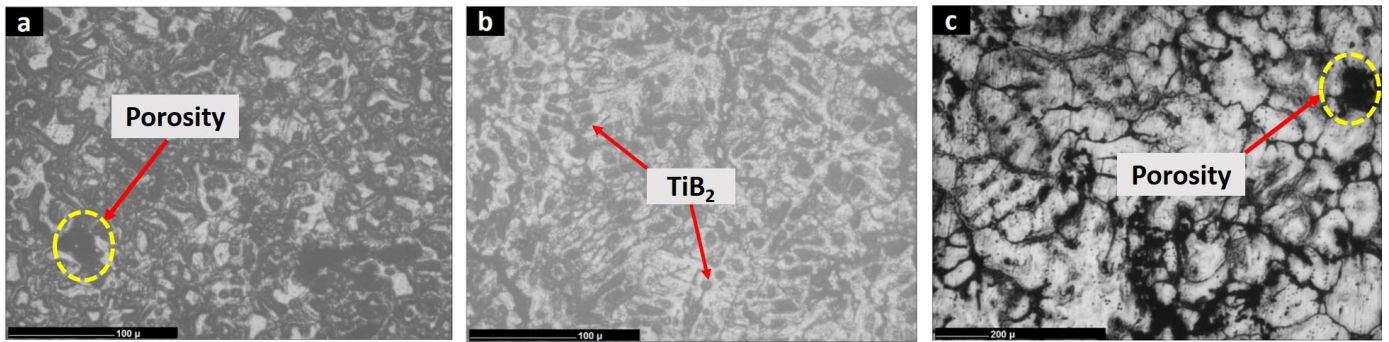


Fig. 6. Influence of stirring time on microstructure (A713+2% TiB₂) composite cast at stirring speed of 700 rpm: (a) 5 min (b) 10 min (c) 15 min

Fig. 7 and Fig. 8 shows the how the stirring speed and stirring time affected the average grain size of the composites. It is observed that the finest grain size was observed within the composite fabricated at 600 rpm stirring speed and 10 min stirring time.

3.2. XRD analysis

Fig. 9 depicts the X-ray diffraction (XRD) patterns of stir-cast matrix A713 alloy and A713-TiB₂ composite. A 2θ range

of 10-80 degrees is used to measure diffraction intensity peaks. The XRD analysis demonstrates the existence of peaks corresponding to aluminium and TiB₂. It shows that there are no any peaks found due to interfacial reaction compounds. This is due to the exceptional stability of TiB₂ particles into molten matrix and also it does not produce reactive elements at the interface [38]. Thus, the addition of reinforcement particles does not affects the existing phases and the performance of the composite [39].

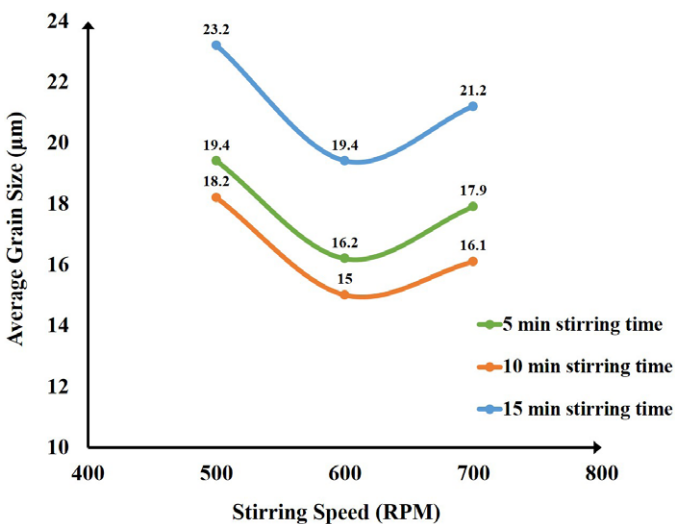


Fig. 7. Influence of stirring speed on average grain size of cast A713-TiB₂ MMCs

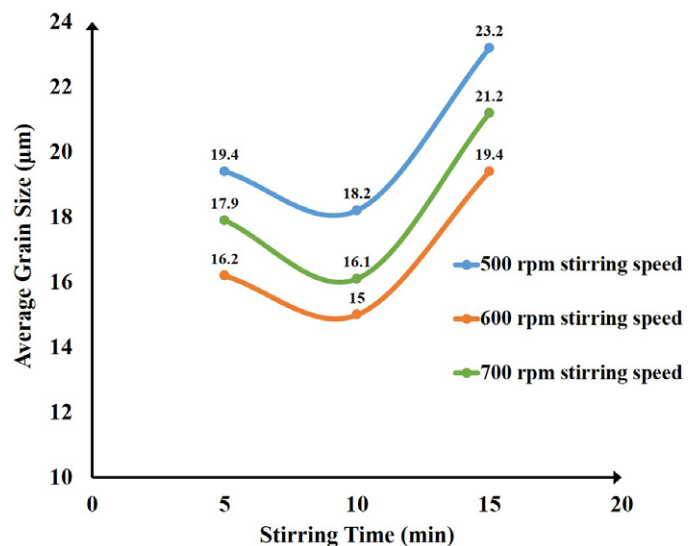


Fig. 8. Influence of stirring time on average grain size of cast A713-TiB₂ MMCs

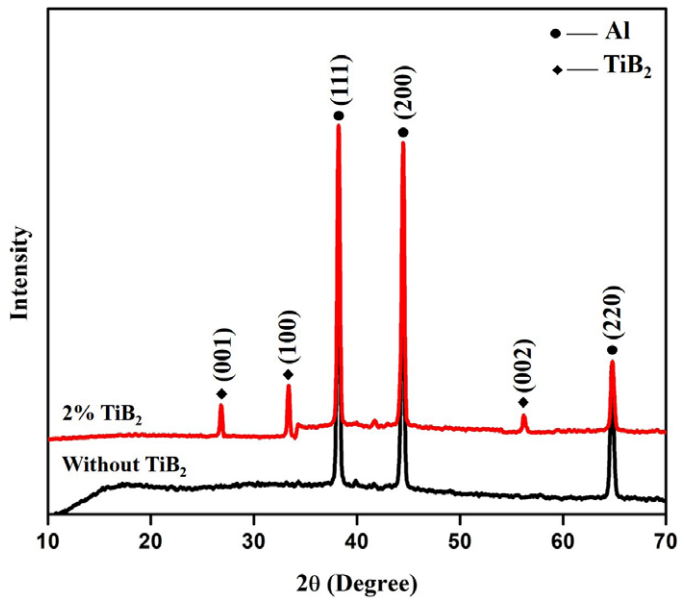


Fig. 9. XRD pattern of fabricated Al-TiB₂ composite cast at stirring speed of 600 rpm and 10 min stirring time

3.3. Micro-hardness

Average microhardness values of Al/TiB₂ composites at different levels of parameters are shown in Fig. 10. Microhardness testing was performed in accordance with ASTM E-18 standards. When TiB₂ is added into the alloy matrix, the hardness significantly improves. Increased hardness shows that incorporating TiB₂ particles into the aluminium matrix has resulted in improved composite hardness. This is because aluminium matrix is a soft and flexible metallic material, and the reinforced particle, notably ceramics material, is a hard material. The combination of these two in one leads to a second phase strengthening mechanism of the particle reinforcement type. Due to particle reinforcement the hardness of the composites is observed higher than cast alloy A713. Adding harder and rigid TiB₂ reinforcement makes the matrix more resistant to plastic deformation during a hardness test [40]. Therefore, the comparatively high hardness of TiB₂ itself might be responsible for the rise in overall hardness of the composite. In addition there is also role of grain size reduction. Noted data of microhardness can be correlated with measured grain size. It is clear that microhardness increases as grain size decreases.

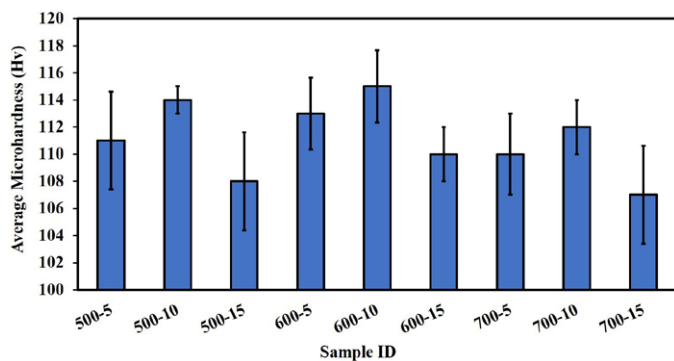


Fig. 10. Average micro-hardness of cast composites

It has been observed from the Fig. 11 that the cast composite made at 500 rpm & 5 min stirring time has hardness value of 111 HV. At 600 rpm, the hardness value reaches its maximum of 113 HV; however, when the speed of the stirring is increased to 700 rpm, the hardness value falls to 110 HV. Therefore, it is clear that raising the speed of the stirrer over 600 rpm does not result in a noticeable increase in the hardness of cast composites.

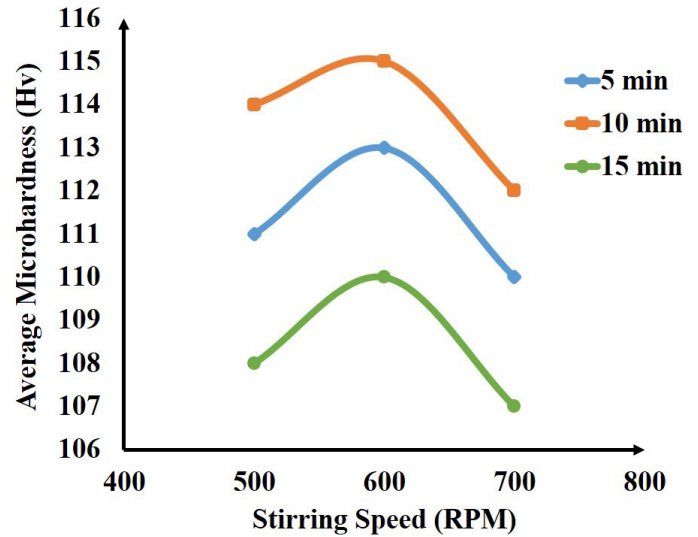


Fig. 11. Influence of stirring speed on average microhardness of cast A713-TiB₂ MMCs

The effect of stirring time is plotted in Fig. 12. The results revealed that at shorter stirring time (5 min) and lower stirring speed (500 rpm), hardness value observed is 111 HV. The hardness value of composite fabricated at 10 min stirring and 500 rpm, is 114 HV. The increasing stirring time to 15 min at the same stirring speed reduces the hardness value (108 HV).

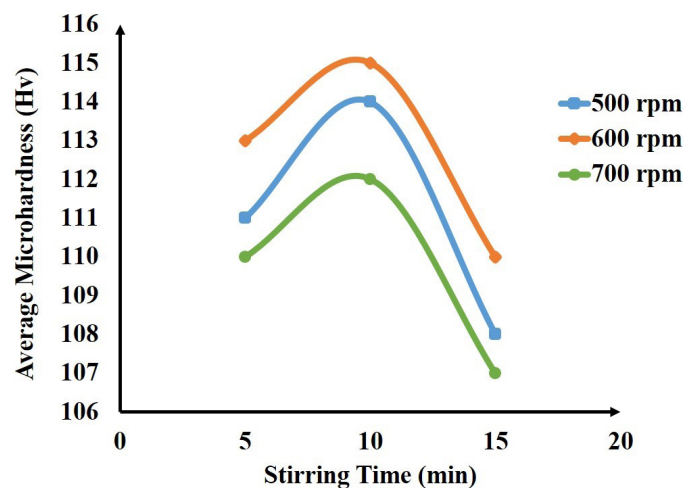


Fig. 12. Influence of stirring time on average microhardness of cast A713-TiB₂ MMCs

It can be concluded from Fig. 10-12 that stirring speed of 600 rpm and stirring time of 10 min yield composites having higher hardness. This is due to uniform distribution of TiB₂

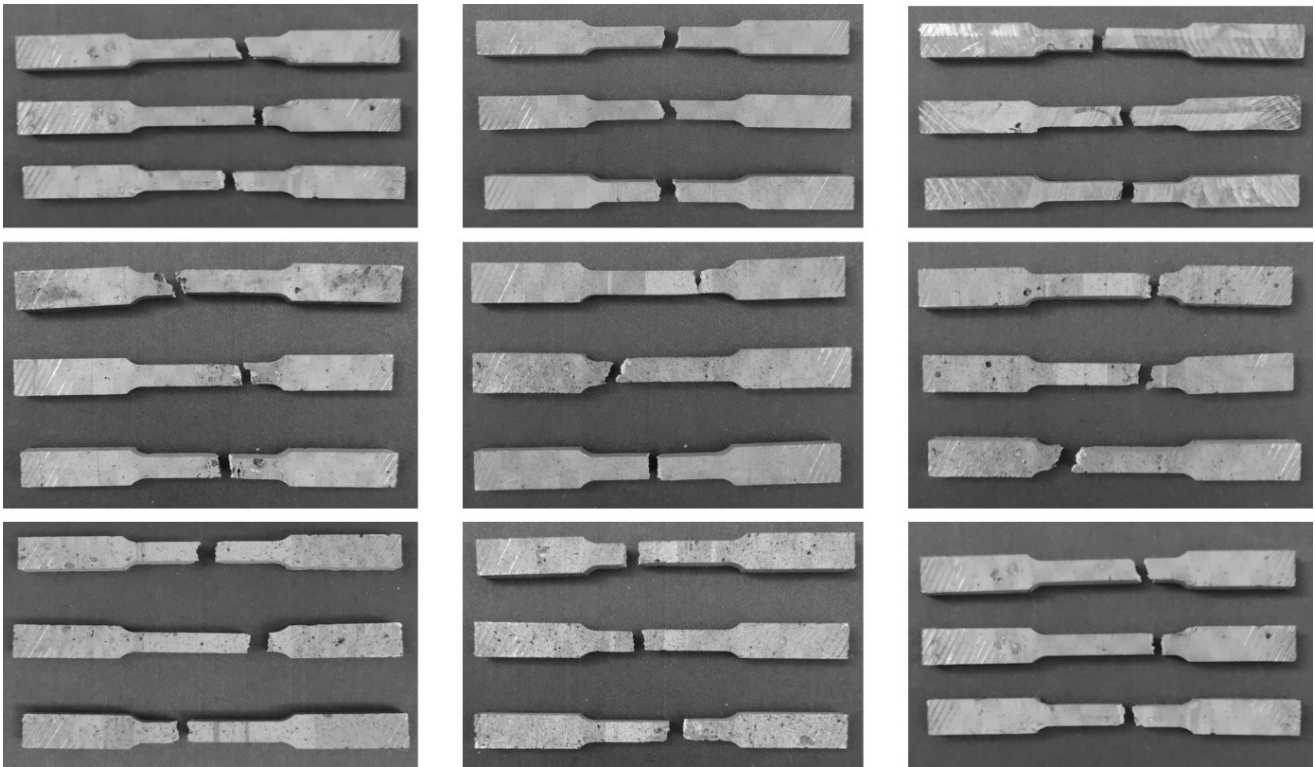


Fig. 13. Tensile test specimens of stir-cast A713-TiB₂ composites after testing

particles in the aluminium matrix. Kennedy et al. [41] have been found a similar trend and reported that increasing both the speed of stirring and stirring time results in a decrease in the hardness of the composites due to the gases formation, porosity formation and any oxide skins.

3.4. Tensile testing

Tensile tests were carried out to investigate the influence of stirring speed and stirring time. The tensile strength of nine cast plates was evaluated. Tensile tests were carried out using a universal testing machine (Model No.: TFUC-200) as per ASTM E8 standard. Test specimens of nine castings after testing are shown in Fig. 13. As evident from tensile strength results, the highest strength obtained in case of 600 rpm stirring speed and

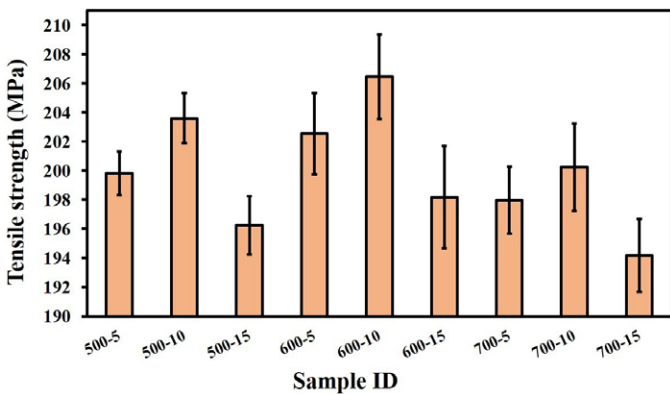


Fig. 14. Tensile strength of cast composites

10 minutes stirring time. It is observed from Fig. 14, the tensile strength improves in conjunction with the speed of stirring and stirring time up to certain limit.

Fig. 15 depicts the influence of stirring speed on the tensile strength of composites. At a stirring speed of 600 rpm, the tensile strength reaches its maximum. Increasing the speed of stirring to 700 rpm decreases tensile strength. A vortex is formed in the aluminium melt, and the supplied particles are dispersed throughout the melt by centrifugal currents created while the stirrer rotates. Creating a vortex is necessary for incorporating the reinforcing particles. However, the extent to which particles are mixed and distributed throughout the melt is constrained

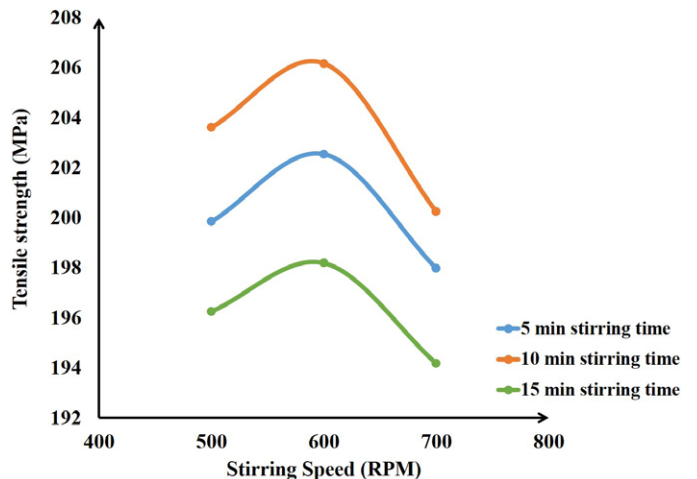


Fig. 15. Influence of stirring speed on tensile strength of stir-cast A713-TiB₂ MMCs

by the size of the vortex created. The stirring should produce circulating currents of sufficient force to maintain the suspension of the particles for a considerable amount of time. The intensity of the circulating current as well as the vortex diameter are both linearly controlled by the amount of time the mixture is stirred. A strong stirring speed and a deep vortex create an entrapment of the air bubbles due to suction and turbulence. This is an unfavourable circumstance that may result in gas to get suck. The impact of stirring speed on tensile behaviour can be better understood using microscopic imaging [42].

The SEM micrographs (Fig. 16) show that the formation of porosity and the dispersion of TiB_2 particles are affected by the stirring speed. At 500 rpm, the distribution is poor and heterogeneous (Fig. 16(a)). Particle-free zones are also identified in some places. At 600 rpm, a more even dispersion of TiB_2 particles are observed in the micrograph (Fig. 16(b)). Increasing the speed of stirring causes a greater centrifugal current inside the aluminium melt, which breaks up any clusters of TiB_2 and disperses the particles evenly throughout the melt. The resulting vortex is the optimal shape for achieving uniform dispersion. At 700 rpm, the micrograph (Fig. 16(c)) reveals that the dispersion of TiB_2 particles in the aluminium matrix is even more uniform. When the stirring speed is raised from 500 to 700 rpm, there are spots

of porosity visible throughout the micrograph. At 700 rpm, the vortex created by the stirring is strong enough to draw air from the atmosphere into the aluminium melt because of the greater pressure differential. The vortex almost approaches top surface of the stirrer blade. This conclusion is consistent with the study done by Ravi et al. [43]. The gas porosities are not noticed at 500 and 600 rpm for a steady 10 minutes of stirring. When solidifying, the increased volume of gas absorbed at 700 rpm does not totally released. Due of the trapped gases, the AMC casting has gas porosity.

A plot of tensile strength against stirring time for cast Al- TiB_2 composites is shown in Fig. 17. As stirring time is increased, the tensile strength rises, with a peak occurring at 10 minutes. The tensile strength decreases as the stirring time increases further. The stirrer's motion generates a vortex, which sucks the particles into the aluminium molten pool. This is because the supplied particles will not instantly spread over the whole aluminium molten pool. According to Prabu, et al. [44], the dispersion is a function of time. In order to evenly distribute the particles throughout the aluminium melt, they must be exposed to continual centrifugal currents for a set amount of time. On the other hand, the vortex tends to draw air into the molten slurry. The stirring time affects the volume of air that

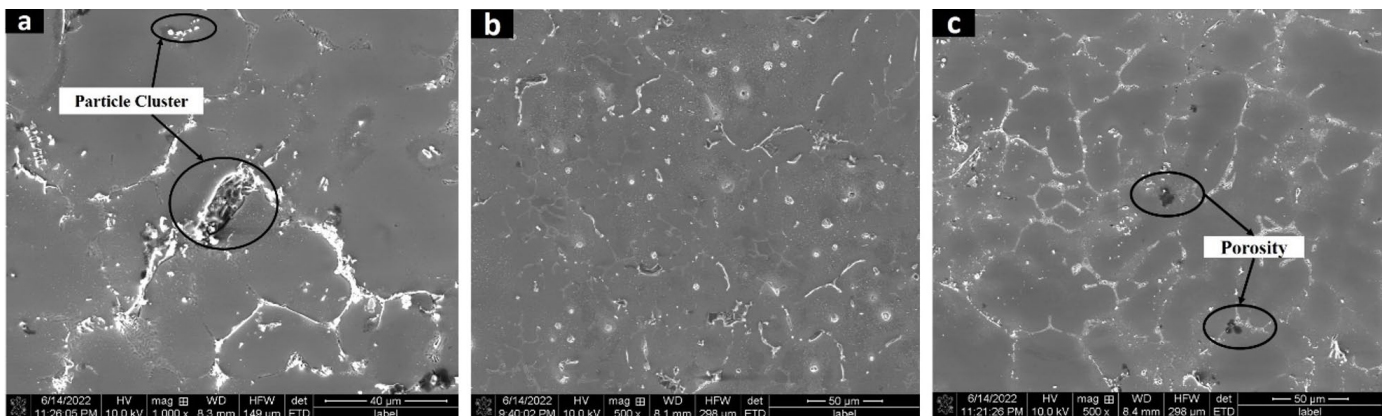


Fig. 16. SEM micrograph of A713- TiB_2 composites fabricated at (a) 500 rpm; (b) 600 rpm; (c) 700 rpm

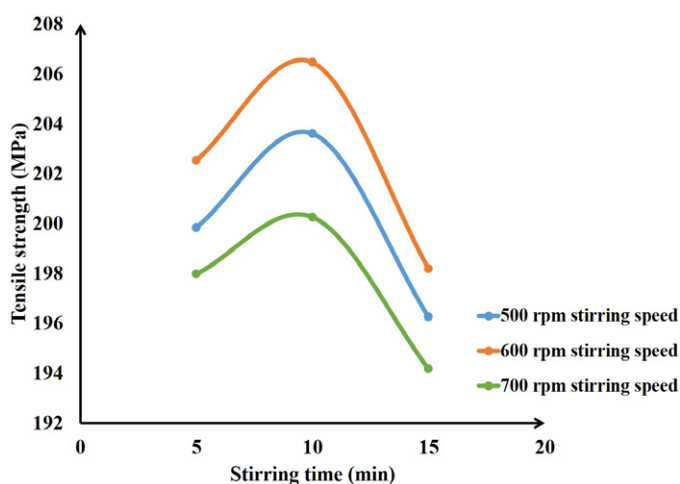


Fig. 17. Influence of stirring time on tensile strength of cast Al- TiB_2 MMCs

is drawn inside the molten slurry. Longer stirring times cause air entrapment and casting porosity. Micrographs (Fig. 18(a)-(c)) show the influence of stirring time on the casting of A713- TiB_2 composites.

The SEM micrographs of A713- TiB_2 composite at different stirring times are shown in Fig. 18(a-c). The micrographs exhibit variation indicating of the influence of stirring time. At 5 minutes of stirring, several clusters can be seen in the microscope (Fig. 18(a)). In addition to this, particle-free zones may be seen. The heterogeneous structure is identified from the micrograph. The TiB_2 particles cannot be evenly distributed in the aluminium matrix with a stirring time of only 5 minutes. The TiB_2 particles in the aluminium melt tend to stick together, forming clusters. At a stirring time of 10 minutes, the micrograph (Fig. 18(b)) reveals that the TiB_2 particles are homogeneously dispersed throughout the aluminium matrix. Particles are dispersed more evenly as stir-

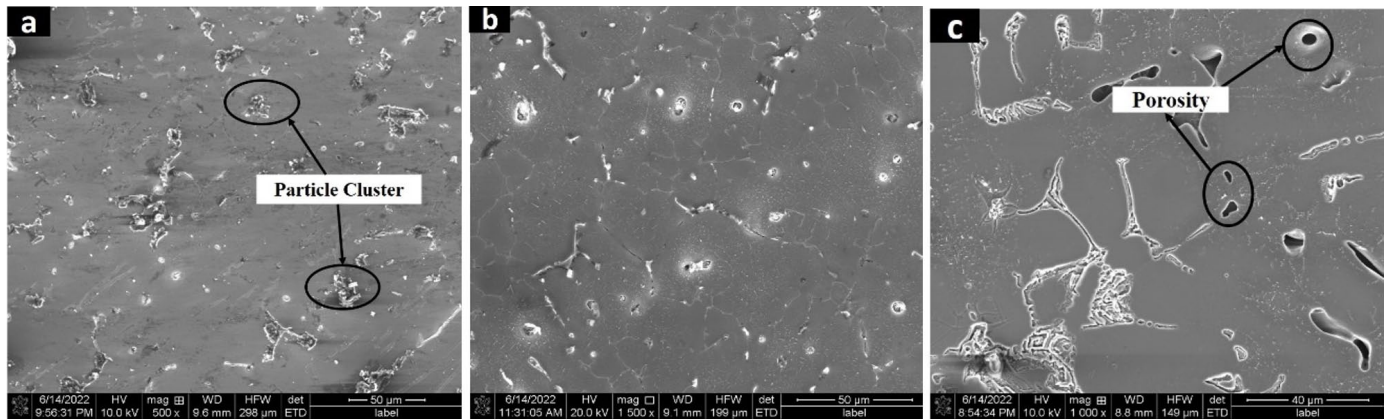


Fig. 18. SEM micrograph of A713-TiB₂ composites fabricated at (a) 5 min; (b) 10 min; (c) 15 min

ring time increases. The clusters of molten aluminium break apart due to centrifugal currents as stirring times increase. The particles that were clustered together are pushed out of the clusters and into particle-free regions. In this way, the dispersion gets better as the stirring continues. At 15 minutes of stirring (Fig. 18(c)), the SEM micrograph shows that the more uniform distribution of TiB₂ particles is observed at the expense of porosity. Increasing the time duration for stirring from 5 minutes to 15 minutes helps the TiB₂ reinforcement to disperse more evenly. Several factors, including gas entrapment during stirring, solidification shrinkage, water vapour on the surface of the ceramic particles, air bubbles entering the composite melt, and hydrogen evolution contribute to the production of porosity in the cast MMCs. A longer period of stirring results in a greater amount of agitation inside the molten composite, which enhances the tendency to generate a greater amount of porosity [45]. Therefore, a longer stirring time will not produce the homogeneous dispersion in the microstructure. The observations demonstrate that there exists an optimum stirring time for achieving a homogeneous dispersion with minimal porosity. When stirring is extended beyond the optimum range, the molten aluminium will have a larger ability to absorb gas. Consequently, porosity formation becomes inevitable. Different porosities occur as a result of gas bubbles forming and growing preferentially during the solidification process.

4. Conclusions

The microscopic examination, XRD analysis, microhardness measurements and tensile testing of composites fabricated at different stirring speeds (500, 600 and 700 rpm) and different stirring time (5, 10 and 15 min) are discussed. The following conclusions were made from the present study: (i) As per the grain size analysis it is observed that the finest grain structure is formed in composites fabricated at 600 rpm stirring speed and 10 min stirring time. XRD analysis has clearly revealed the presence of TiB₂ particles in the composites. (ii) Microhardness results revealed that average microhardness of AMCs fabricated at 600 rpm and 10 min stirring time gives a better result as compared to the same of composites cast at combination of

level of parameters. (iii) The tensile strength was found higher when the porosity was low (composite fabricated at stirring speed of 600 rpm & 10 min stirring time) and distribution was homogenous.

REFERENCES

- [1] A. Ramanathan, P.K. Krishnan, R. Muraliraja, A review on the production of metal matrix composites through stir casting – Furnace design, properties, challenges, and research opportunities. *J. Manuf. Process.* **42**, 213-245(2019). DOI: <https://doi.org/10.1016/j.jmapro.2019.04.017>
- [2] R. Thiraviam, V. Ravisankar, P.K. Krishnan, R. Arunachalam, Microstructural and Mechanical Properties of Al-Reinforced with Micro and Nano Al₂O₃ Particles using Stir-Squeeze Casting Method. *Int. J. Mech. Prod. Eng. Res. Dev.* **10**, 193-202 (2020). DOI: <https://doi.org/10.24247/ijmpredjun202018>
- [3] V. Bhuvaneshwari, L. Rajeshkumar, R. Saravanakumar, D. Balaji, Synthesis and Characterization of Bioceramics Reinforced Aluminium Matrix Composites. *Arch. Metall. Mater.* **67** (4), 1217-1226 (2022). DOI: <https://doi.org/10.24425/amm.2022.141045>
- [4] A.M. Jaber, P.K. Krishnan, Development of a sustainable novel aluminum alloy from scrap car wheels through a stir-squeeze casting process. *Kov. Mater. Mater.* **60** (2022). DOI: <https://doi.org/10.31577/km.2022.3.151>
- [5] J.D.R. Selvam, D.R. Smart, I. Dinaharan, Microstructure and some mechanical properties of fly ash particulate reinforced AA6061 aluminum alloy composites prepared by comocasting. *Mater. Des.* **49**, 28-34 (2013). DOI: <https://doi.org/10.1016/j.matdes.2013.01.053>
- [6] S. Rangrej, S. Pandya, J. Menghani, Effects of TiB₂ reinforcement proportion on structure and properties of stir cast A713 composites, *Can. Metall. Q.* (2022). DOI: <https://doi.org/10.1080/00084433.2022.2149202>
- [7] S. Rangrej, V. Mehta, V. Ayar, M. Sutaria, Effects of stir casting process parameters on dispersion of reinforcement particles during preparation of metal composites. *Mater. Today: Proc.* **43**, 471-475 (2021). DOI: <https://doi.org/10.1016/j.matpr.2020.11.1002>

- [8] R. Thiraviam, V. Ravisankar, P. Kumar, R. Thanigaivelan, R. Arunachalam, A novel approach for the production and characterisation of aluminium–alumina hybrid metal matrix composites. *Mater. Res. Express.* **7** (4), 046512 (2020). DOI: <https://doi.org/10.1088/2053-1591/ab8657>
- [9] Z.Y. Liu, D. Kent, G.B. Schaffer, Powder injection moulding of an Al–AlN metal matrix composite. *Mater. Sci. Eng. A.* **513**, 352-356 (2009). DOI: <https://doi.org/10.1016/j.msea.2009.02.001>
- [10] H. Mindivan, Reciprocal sliding wear behaviour of B₄C particulate reinforced aluminum alloy composites. *Mater. Lett.* **64**(3), 405-407 (2010). DOI: <https://doi.org/10.1016/j.matlet.2009.11.032>
- [11] R. Arunachalam, P.K. Krishnan, Compressive Response of Aluminum Metal Matrix Composites, in: *Encyclopedia of Materials: Composites*. Elsevier Ltd., 1-21(2021). DOI: <https://doi.org/10.1016/B978-0-12-803581-8.11818-1>
- [12] M.A. Moghaddas, S.F. Kashani-Bozorg, Effects of thermal conditions on microstructure in nanocomposite of Al/Si₃N₄ produced by friction stir processing. *Mater. Sci. Eng. A.* **559**, 187-193 (2013). DOI: <https://doi.org/10.1016/j.msea.2012.08.073>
- [13] Q. Wu, C. Yang, F. Xue, Y. Sun, Effect of Mo addition on the microstructure and wear resistance of in situ TiC/Al composite. *Mater. Des.* **32** (10), 4999-5003 (2011). DOI: <https://doi.org/10.1016/j.matdes.2011.06.045>
- [14] I. Dinaharan, N. Murugan, Dry sliding wear behavior of AA6061/ZrB₂ in-situ composite. *Trans. Nonferrous Met. Soc. China.* **22** (4), 810-818 (2012). DOI: [https://doi.org/10.1016/S1003-6326\(11\)61249-1](https://doi.org/10.1016/S1003-6326(11)61249-1)
- [15] V. Mohanavel, Mechanical and microstructural characterization of AA7178-TiB₂ composites. *Mater. Test.* **62** (2), 146-150 (2020). DOI: <https://doi.org/10.3139/120.111465>
- [16] Y. Pazhuhanfar, B. Eghbali, Processing and characterization of the microstructure and mechanical properties of Al6061-TiB₂ composite. *Int. J. Miner. Metall.* **28** (6), 1080-1089 (2021). DOI: <https://doi.org/10.1007/s12613-021-2288-0>
- [17] S. Yadav, A. Aggrawal, A. Kumar, K. Biswas, Effect of TiB₂ addition on wear behavior of (AlCrFeMnV) 90Bi10 high entropy alloy composite. *Tribol. Int.* **132**, 62-74 (2019). DOI: <https://doi.org/10.1016/j.triboint.2018.11.025>
- [18] K.L. Tee, L. Lu, M.O. Lai, Synthesis of in situ Al–TiB₂ composites using stir cast route. *Compos. Struct.* **47** (1-4), 589-593 (1999). DOI: [https://doi.org/10.1016/S0263-8223\(00\)00030-1](https://doi.org/10.1016/S0263-8223(00)00030-1)
- [19] R. Muraliraja, K. Pradeepkumar, P. Mohanraj, T.V. Kumar, C. Dhanasekaran, M. Chandrasekaran, S. Ragavanantham, V.S. Shaisundaram, The Effects of Electroless Ni-P Coated SiC on the Properties of Magnesium Composite. *Mater. Perform. Charact.* **11** (1), 223-235 (2022). DOI: <https://doi.org/10.1520/MPC20210089>
- [20] D. Paulraj, P.D. Jeyakumar, G. Rajamurugan, P. Krishnasamy, Influence of Nano TiO₂/Micro (SiC/B₄C) reinforcement on the mechanical, wear and corrosion behaviour of A356 metal matrix composite. *Arch. Metall. Mater.* **66** (3), 871-880 (2021). DOI: <https://doi.org/10.24425/amm.2021.136392>
- [21] A.M. Sankhla, K.M. Patel, M.A. Makhesana, K. Giasin, D.Y. Pimenov, S. Wojciechowski, N. Khanna, Effect of mixing method and particle size on hardness and compressive strength of aluminium based metal matrix composite prepared through powder metallurgy route. *J. Mater. Res. Technol.* **18**, 282-292 (2022). DOI: <https://doi.org/10.1016/j.jmrt.2022.02.094>
- [22] S. Rangrej, S. Pandya, J. Menghani, Effects of reinforcement additions on properties of aluminium matrix composites – a review. *Mater. Today: Proc.* **44**, 637-641 (2021). DOI: <https://doi.org/10.1016/j.matpr.2020.10.604>
- [23] M.A. Taha, Practicalization of cast metal matrix composites (MMCCs). *Mater. Des.* **22** (6), 431-441 (2001). DOI: [https://doi.org/10.1016/S0261-3069\(00\)00077-7](https://doi.org/10.1016/S0261-3069(00)00077-7)
- [24] J. Hashim, L. Looney, M.S.J. Hashmi, Particle distribution in cast metal matrix composites – Part I. *J. Mater. Process. Technol.* **123**(2), 251-257 (2002). DOI: [https://doi.org/10.1016/S0924-0136\(02\)00098-5](https://doi.org/10.1016/S0924-0136(02)00098-5)
- [25] R. Arunachalam, S. Piya, P.K. Krishnan, R. Muraliraja, J.V. Christy, A.H.I. Mourad, M. Al-Maharbi, Optimization of stir–squeeze casting parameters for production of metal matrix composites using a hybrid analytical hierarchy process–Taguchi-Grey approach. *Eng. Optim.* **52**(7), 1166-1183(2019). DOI: <https://doi.org/10.1080/0305215X.2019.1639693>
- [26] S.B. Prabu, L. Karunamoorthy, S. Kathiresan, B. Mohan, Influence of stirring speed and stirring time on distribution of particles in cast metal matrix composite. *J. Mater. Process. Technol.* **171** (2), 268-273 (2006). DOI: <https://doi.org/10.1016/j.jmatprotec.2005.06.071>
- [27] J. Hashim, L. Looney, M.S.J. Hashmi, The enhancement of wettability of SiC particles in cast aluminium matrix composites. *J. Mater. Process. Technol.* **119** (1-3), 329-335 (2001). DOI: [https://doi.org/10.1016/S0924-0136\(01\)00919-0](https://doi.org/10.1016/S0924-0136(01)00919-0)
- [28] G. Sasaki, M. Yoshida, N. Fuyama, T. Fujii, Modeling of compocasting process and fabrication of AZ91D magnesium alloy matrix composites. *J. Mater. Process. Technol.* **130**, 151-155 (2002). DOI: [https://doi.org/10.1016/S0924-0136\(02\)00712-4](https://doi.org/10.1016/S0924-0136(02)00712-4)
- [29] P.K. Krishnan, R. Arunachalam, A. Husain, M. Al-Maharbi, Studies on the influence of stirrer blade design on the microstructure and mechanical properties of a novel aluminum metal matrix composite. *J. Manuf. Sci. Eng. Trans. ASME* **143**, 1-13 (2021). DOI: <https://doi.org/10.1115/1.4048266>
- [30] G. Sozhamannan, S. Prabu, V. Venkatagalapathy, Effect of processing parameters on metal matrix composites: Stir casting process. *J. Surf. Eng. Mater. Adv. Technol.* **2**, 11-15 (2012). DOI: <https://doi.org/10.4236/jsemat.2012.21002>
- [31] H. Zhang, L. Geng, L. Guan, L. Huang, Effects of SiC particle pretreatment and stirring parameters on the microstructure and mechanical properties of SiC_p/Al–6.8 Mg composites fabricated by semi-solid stirring technique. *Mater. Sci. Eng. A.* **528** (1), 513-518 (2010). DOI: <https://doi.org/10.1016/j.msea.2010.09.046>
- [32] L.N. Guan, G. Lin, H.W. Zhang, L.J. Huang, Effects of stirring parameters on microstructure and tensile properties of (ABO_w+SiC_p)/6061Al composites fabricated by semi-solid stirring technique. *Trans. Nonferrous Met. Soc. China.* **21**, 274-279 (2011). DOI: [https://doi.org/10.1016/S1003-6326\(11\)61590-2](https://doi.org/10.1016/S1003-6326(11)61590-2)
- [33] M.K. Akbari, O. Mirzaee, H.R. Baharvandi, Fabrication and study on mechanical properties and fracture behavior of nanometric

- Al_2O_3 particle-reinforced A356 composites focusing on the parameters of vortex method. *Mater. Des.* **46**, 199-205 (2013).
DOI: <https://doi.org/10.1016/j.matdes.2012.10.008>
- [34] H. Khosravi, H. Bakhshi, E. Salahinejad, Effects of compocasting process parameters on microstructural characteristics and tensile properties of A356– SiC_p composites. *Trans. Nonferrous Met. Soc. China.* **24**(8), 2482-2488 (2014).
DOI: [https://doi.org/10.1016/S1003-6326\(14\)63374-4](https://doi.org/10.1016/S1003-6326(14)63374-4)
- [35] P.K. Krishnan, J.V. Christy, R. Arunachalam, A.H.I. Mourad, R. Muraliraja, M. Al-Maharbi, V. Murali, M.M. Chandra, Production of aluminium alloy-based metal matrix composites using scrap aluminum alloy and waste materials: Influence on microstructure and mechanical properties. *J. Alloys Compd.* **784**, 1047-1061(2019).
DOI: <https://doi.org/10.1016/j.jallcom.2019.01.115>
- [36] A.I. Mourad, J. Victor, P.K. Krishnan, Production of novel recycled hybrid metal matrix composites using optimized stir squeeze casting technique. *J. Manuf. Process.* **88**, 45-58 (2023).
DOI: <https://doi.org/10.1016/j.jmapro.2023.01.040>
- [37] H.M. Rajan, S. Ramabalan, I. Dinaharan, S.J. Vijay, Effect of TiB_2 content and temperature on sliding wear behavior of AA7075/ TiB_2 in situ aluminum cast composites. *Arch. Civ. Mech. Eng.* **14** (1), 72-79 (2014).
DOI: <https://doi.org/10.1016/j.acme.2013.05.005>
- [38] B.S. Murty, S.A. Kori, M. Chakraborty, Grain refinement of aluminium and its alloys by heterogeneous nucleation and alloying. *Int. Mater. Rev.* **47** (1), 3-29 (2002).
DOI: <https://doi.org/10.1179/095066001225001049>
- [39] J.V. Christy, R. Arunachalam, A.H.I. Mourad, P.K. Krishnan, S. Piya, M. Al-Maharbi, Processing, Properties, and Microstructure of Recycled Aluminum Alloy Composites Produced Through an Optimized Stir and Squeeze Casting Processes. *J. Manuf. Process.* **59**, 287-301 (2020).
DOI: <https://doi.org/10.1016/j.jmapro.2020.09.067>
- [40] S. Charles, V.P. Arunachalam, Effect of particle inclusions on the mechanical properties of composites fabricated by liquid metallurgy. *Indian J. Eng. Mater. Sci.* **10**, 301-305 (2003).
DOI: <http://nopr.niscares.in/handle/123456789/24213>
- [41] A.R. Kennedy, A.E. Karantzalis, S.M. Wyatt, The microstructure and mechanical properties of TiC and TiB_2 -reinforced cast metal matrix composites. *J. Mater. Sci.* **34** (5), 933-940 (1999).
DOI: <https://doi.org/10.1023/A:1004519306186>
- [42] J.J. Moses, I. Dinaharan, S.J. Sekhar, Prediction of influence of process parameters on tensile strength of AA6061/TiC aluminum matrix composites produced using stir casting. *Trans. Nonferrous Met. Soc. China.* **26**(6), 1498-1511 (2016).
DOI: [https://doi.org/10.1016/S1003-6326\(16\)64256-5](https://doi.org/10.1016/S1003-6326(16)64256-5)
- [43] K.R. Ravi, V.M. Sreekumar, R.M. Pillai, C. Mahato, K.R. Amaranathan, B.C. Pai, Optimization of mixing parameters through a water model for metal matrix composites synthesis. *Mater. Des.* **28** (3), 871-881 (2007).
DOI: <https://doi.org/10.1016/j.matdes.2005.10.007>
- [44] S.B. Prabu, L. Karunamoorthy, S. Kathiresan, B. Mohan, Influence of stirring speed and stirring time on distribution of particles in cast metal matrix composite. *J. Mater. Process. Technol.* **171** (2), 268-273 (2006).
DOI: <https://doi.org/10.1016/j.jmatprotec.2005.06.071>
- [45] M.K. Akbari, O. Mirzaee, H.R. Baharvandi, Fabrication and study on mechanical properties and fracture behavior of nanometric Al_2O_3 particle-reinforced A356 composites focusing on the parameters of vortex method. *Mater. Des.* **46**, 199-205 (2013).
DOI: <https://doi.org/10.1016/j.matdes.2012.10.008>